ACS OMEGA

Open Access

http://pubs.acs.org/journal/acsodf

Article

Effects of Surfactants on Oil Droplet Demulsification in Oil-in-Water Emulsions under an Electric Field: A Molecular Dynamics Study

Shasha Liu,* Heng Zhang, Shideng Yuan, and Shiling Yuan*

Cite This: *ACS Omega* 2024, 9, 48232−48245

Read Online

ACCESS | Metrics & More | Article Recommendations | Supporting Information

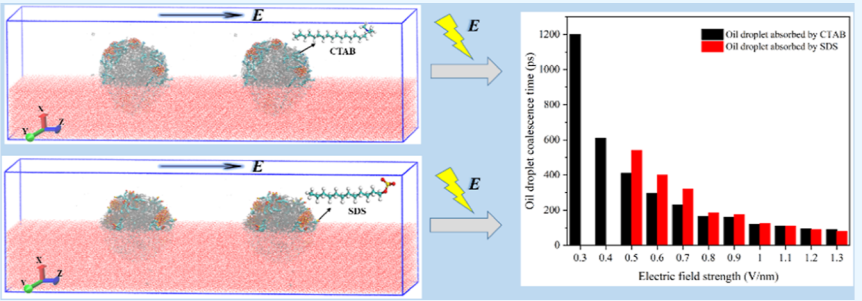

ABSTRACT: The application of an electric field to demulsification of oil-in-water (O/W) emulsions has received extensive attention. However, microcosmic information about the effect of surfactant type on the demulsification of an O/W emulsion under an electric field is still rare. In this work, the effects of cationic surfactant cetyltrimethylammonium bromide (CTAB) and anionic surfactant sodium dodecyl sulfate (SDS) on oil droplet demulsification in an emulsion under a pulsed-DC electric field were studied by molecular dynamics (MD) simulation. The MD simulation results show that oil droplets underwent directional movement under the action of an electric field. The larger the electric field strength, the shorter the time required for the oil droplets to coalesce. However, the movement direction of the oil droplets in the electric field was different depending on the type of surfactant. Compared to oil droplets containing SDS, oil droplets containing CTAB molecules exhibited faster deformation and easier migration coalescence under low electric field strength. It was mainly attributed to the fact that the deformation of oil droplets will be accelerated when oil droplets contain asphaltene molecules and surfactant molecules with different electronegativities under an electric field. During the demulsification of oil droplets containing CTAB molecules, CTAB molecules generated electrostatic attraction with asphaltene molecules in adjacent oil droplets, strengthened the interaction between oil droplets, and promoted the demulsification of oil droplets. In the process of oil droplet demulsification containing SDS molecules, the potential energy of the electrostatic interaction between oil droplets did not change, and the demulsification mainly depended on the van der Waals force between oil droplets.

1. INTRODUCTION

Due to the strong mixing of the oil phase and water phase during the extraction, gathering, and transportation of crude oil, the produced liquid of crude oil often exists in the form of an emulsion. Crude oil emulsions contain surface-active components, such as asphaltenes and resins, which naturally exist in crude oil. In addition, most oil fields produce solid nanoparticles during the oil recovery process, such as silica, produced clay minerals,[1,2] and fine carbonate.[3,4] These natural surfactants will also promote the stability of the emulsions by forming highly viscous or rigid interfacial films between the oil and water. With the maturation of tertiary oil recovery technology, chemical oil flooding, represented by surfactant flooding, has become the mainstream oil displacement technology. The commonly used surfactants for oil recovery are anionic surfactants [such as sodium dodecyl sulfate (SDS)] and cationic surfactants [such as cetyltrimethylammonium bromide (CTAB)], or nanomaterials obtained by combining them with other materials to enhance oil recovery efficiency.[5,6] As a widely used EOR technique, surfactant flooding not only improves oil recovery but also brings about oil emulsification.[7−10] Meanwhile, the emulsions are very stable in the presence of the injected surfactants.

At present, there are methods to separate oil and water, such as chemical, biological, and physical treatment. It is found that the electric field can evidently influence the morphology of a microstructure of droplets.[11] In water-in-oil (W/O) emulsions, the application of an electric field can cause the polarization or migration of water droplets. The two potential mechanisms

Received: June 15, 2024
Revised: November 14, 2024
Accepted: November 18, 2024
Published: November 26, 2024

may promote coalescence between two water droplets, thereby achieving the demulsification effect.[12] Meanwhile, research has found that AC, DC, pulsed-DC fields, and their combinations have good demulsification effects on W/O emulsions.[12−19] In addition, Ren and Kang[20] applied the pulsed-DC field to separate O/W emulsions and found that the pulsed-DC field induced the aggregation of oil droplets. Therefore, the pulsed-DC electric field is also applicable to the O/W emulsion demulsification. The electric field method also has the advantages of environmental friendliness and low energy consumption.

Base on the universality of surfactants in emulsions, some researchers have experimentally studied the coalescence of emulsion droplets in the presence of surfactants under an applied electric field. Zhang et al.[21] investigated the effect of surfactants on the deformation and fragmentation of water droplets in oil by applying an electric field to the emulsion. They found that the presence of surfactants affected the degree of deformation and the pattern of fragmentation. Yang et al.[22] added a nonionic surfactant to the sunflower seed oil−water emulsion to explore the effect of the surfactant on the partial coalescence of water droplets at the oil−water interface under different electric fields. The results indicate that surfactants can adsorb at the oil/water interface, reduce interfacial tension, and improve the deformation ability of coalesced droplets. Mizoguchi and Muto[23] found that surfactants could increase the size of oil droplets in O/W emulsions and promote emulsion demulsification under the action of an electric field. Ren and Kang[20] proposed a redistribution model of the surface charge of oil droplets under a pulsed-DC field and found that oil droplets containing SDS in the O/W emulsion could improve the demulsification effect under the electric field. Some characteristic quantities or physical models from these works can help researchers understand the effects of the electric field used by surfactant-stabilized water droplet coalescence or emulsion demulsification. However, the mechanism of the effect of surfactant types on the demulsification of oil droplets in the O/W emulsion system is not clear, and further systematic study is needed.

Molecular dynamics (MD) simulation is an effective method for studying microscopic physical phenomena, such as molecular adsorption and droplet aggregation. In recent years, many research studies have reported on exploring the micromechanisms of droplet deformation, fragmentation, and coalescence in W/O emulsions under an external electric field through MD simulations.[24−30] However, many work contents mainly focused on the effects of electric field strength,[24,31,32] electric field type,[33,34] and ion concentration[34] on droplets' coalescence behavior. In addition, Qi et al.[35] investigated the inorganic salt concentration and types on electrophoretic migration of oil droplets in O/W emulsions with MD; the results show a decrease in the electrophoretic mobility and deformation of the oil droplets with the increase of ion concentration. Wang et al.[36] studied the demulsification probability of O/W emulsions stabilized by SDS surfactants in electric fields and the deformation and coalescence of two oil droplets under electric fields by using the MD simulation method. According to the simulated results, the configuration and movement of SDS were determined by interactions between SDS molecules themselves and between SDS and oil/water molecules along with the force exerted by the applied electrical field. Qi et al.[37] explored the electrophoretic coalescence behavior of oil droplets containing the SDS surfactant under a DC electric field based on MD simulations. Its results show that the appropriate addition of surfactants can effectively improve the demulsification process of the O/W emulsion in an electric field. However, the comparative study on the demulsification behavior of an O/W emulsion under an electric field between anionic and cationic surfactants at the molecular level is lacking.

In this article, the MD simulation method was used to compare the behavioral differences between the oil droplets adsorbed by SDS molecules and the oil droplets adsorbed by CTAB molecules in pulsed-DC electric fields. Meanwhile, the demulsification mechanism of oil droplets composed of oil molecules, surfactants, and solid particles under the action of a pulsed-DC electric field was studied. First, we constructed oil droplets containing SiO_2 nanoparticles, then constructed two types of emulsified oil droplets adsorbed by SDS and CTAB molecules on this basis, and compared the structural differences of the two emulsified oil droplets. Second, the behavior and demulsification mechanism of the two types of oil droplets under a pulsed-DC electric field were studied. This paper mainly considered the effect of the electric field strength and surfactant type on oil droplet coalescence. We expect that this work will be helpful to the practical application in the petroleum industry and chemical industry.

2. SIMULATION METHOD

2.1. Simulation Force Field and Method. In this study, we used GROMOS54a7 force field parameters[38] to perform MD simulation and analysis. We employed Materials Studio software to construct silica crystals and obtained SiO_2 nanoparticle models through cutting. The force field parameter files and the molecular optimized geometric structures of SiO_2 nanoparticles, SDS, CTAB, asphaltenes, resins, and other hydrocarbons were generated by the Automated Topology Builder (ATB).[39,40] The simple point charge model was selected for the water molecules. The parameters of sodium ions (Na^+) and chloride ions (Cl^-) that neutralize the negative charge have been discussed in the literature.[41]

The periodic boundary condition was applied along all dimensions in all simulations.[42] The fastest conjugate gradient method was the method to minimize the total energy, and the convergence standard was set to less than 1000 kJ $mol^{-1}\cdot nm^{-1}$. In *NVT* and *NPT* ensembles, a velocity rescaling thermostat was used to maintain the system temperature at 298 K with a coupling constant of 0.1 ps. In the *NPT* ensemble, the ambient pressure was executed at 0.1 MPa by the Berendsen method with a coupling time constant of 1.0 ps for each system. During our simulations, bond lengths were constrained by the LINCS algorithm.[43] The van der Waals interaction used a Lennard-Jones 12-6 potential, and the cutoff was set to 1.4 nm. The particle-mesh Ewald summation method was used to calculate the Coulomb interaction.[44,45] Initial velocities were assigned according to the Maxwell−Boltzmann distribution. The time step of simulations was set as 1 fs, and the trajectory was saved every 10 ps. All MD simulations were performed by using the CROMACS software package. The VMD software was used to visualize the computational results.[46] The expression of the external pulsed-DC electric field is

$$E(t) = E_o \exp\left[-\frac{(t - t_0)^2}{2\sigma^2}\right]\cos[\omega(t - t_0)]$$

https://doi.org/10.1021/acsomega.4c05623
ACS Omega 2024, 9, 48232−48245

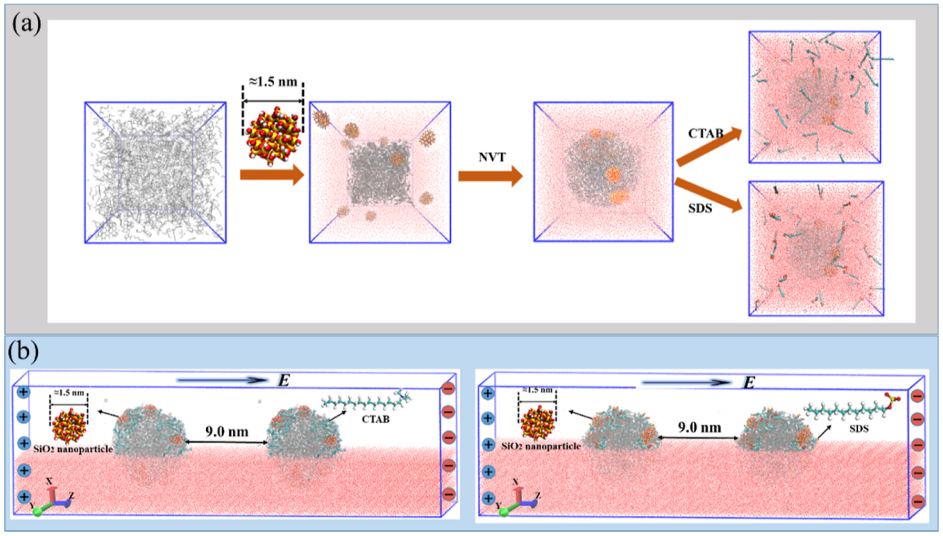

Figure 1. (a) Construction process of the oil droplets adsorbed with surfactants. (b) Initial models of the two emulsion systems under an electric field.

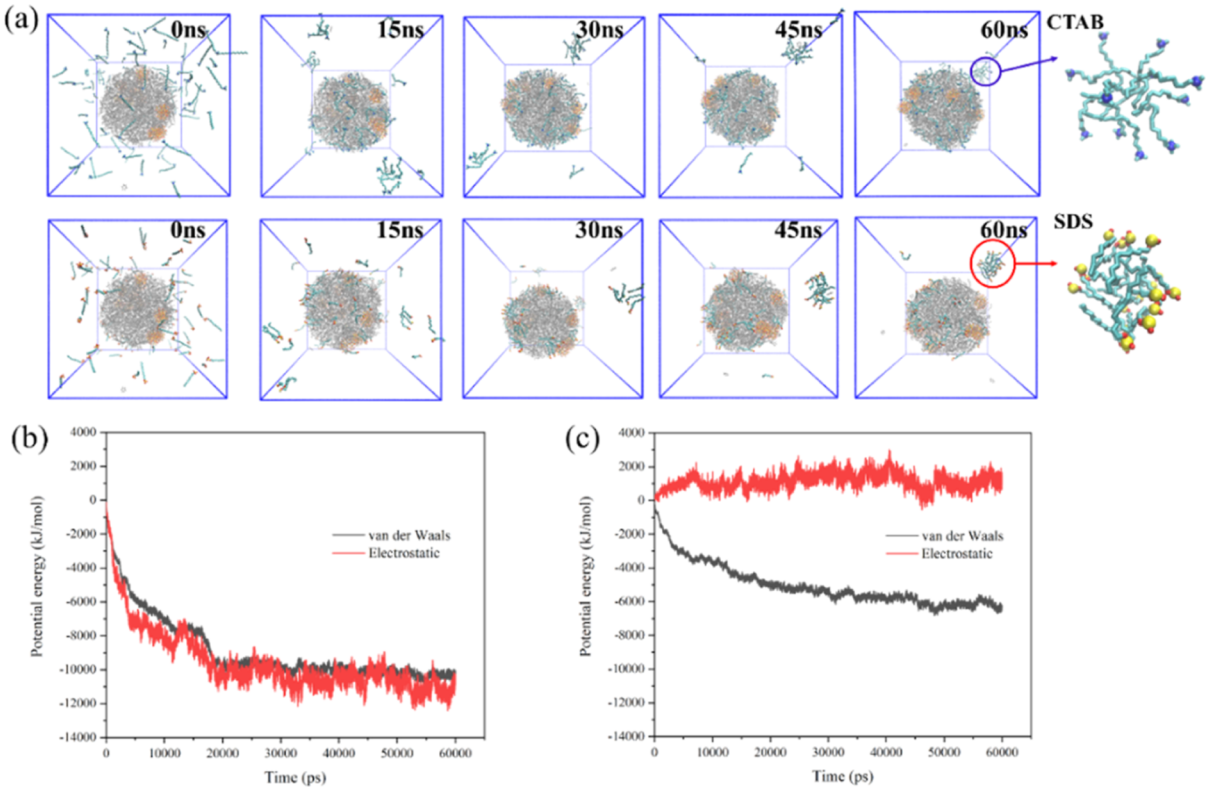

Figure 2. (a) Process of surfactant adsorption on the surface of oil droplets. (b) Potential energy of the interaction between the oil droplets and CTAB surfactants. (c) Potential energy of the interaction between the oil droplets and SDS surfactants.

where t_0 is the maximum time point of the pulse, σ is the pulse width, and ω is the pulse angular frequency. We set σ to 0 to ignore the exponential term and set ω to 0. Meanwhile, based on the setting of electric field strength parameters in multiple papers using the MD method to simulate the demulsification behavior of water droplets or oil droplets under the action of an electric field,[24,27,28,30−36] we set E_o as 0.3, 07, and 1.2 in order to explore the effect of electric field strength on oil droplet demulsification in an O/W emulsion.

2.2. Simulation Model. Crude oil is an extremely complex multicomponent mixture; its heavy components are composed of asphaltenes and resins, and its light components are composed of benzene, cyclic hydrocarbons, and other hydrocarbons. Based on the research studies of Zhang et al. and Song et al.,[47−49] we selected three types of asphaltenes and six types of resins, as well as various hydrocarbons and a small amount of SiO_2 nanoparticles, to form our oil droplet model. The types and quantities of the selected molecules are shown in Figure S1 and Table S1. In order to compare the effects of different types of surfactants on the demulsification process of oil droplets under an electric field, we first constructed nanoparticles containing oil droplets, then constructed two

https://doi.org/10.1021/acsomega.4c05623
ACS Omega 2024, 9, 48232−48245

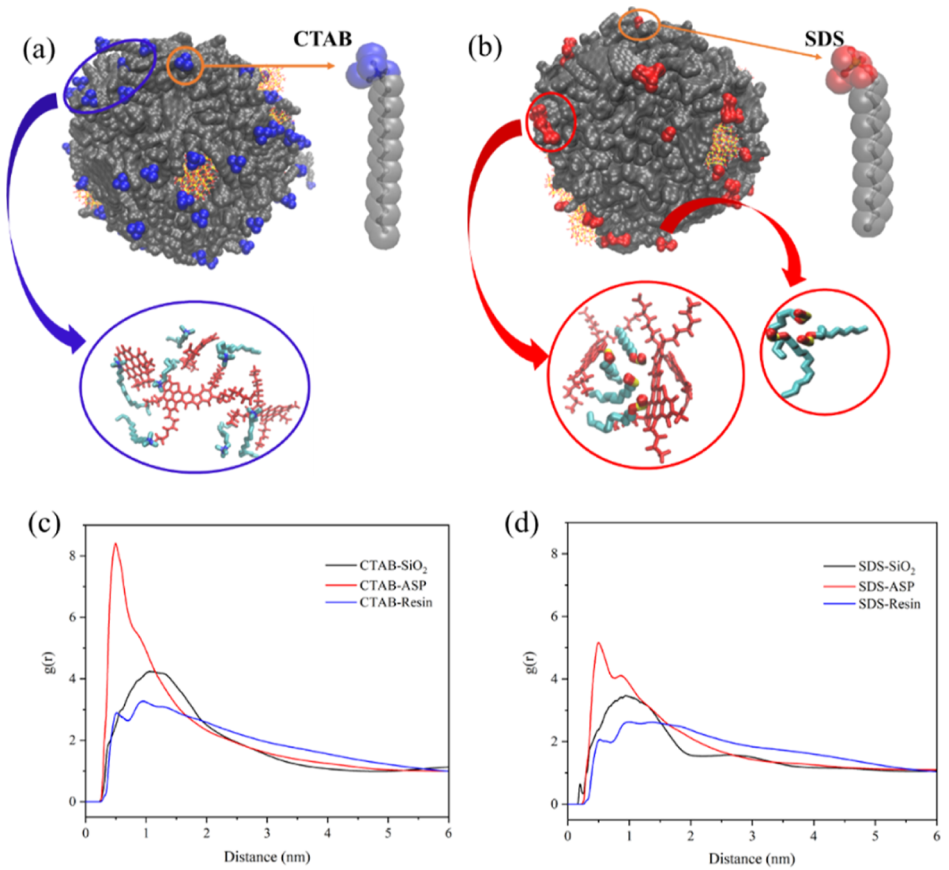

Figure 3. Color schemes and RDF: (a) oil droplet absorbed by CTAB molecules; (b) oil droplet absorbed by SDS molecules; (c) RDF between CTAB molecules and SiO_2 nanoparticles, asphaltene molecules, and resin molecules; and (d) RDF between SDS molecules and SiO_2 silica nanoparticles, asphaltene molecules, and resin molecules.

new simulated boxes of dimension 13 × 13 × 13 nm^3, and placed the oil droplets in the center of the two boxes. Next, 90 SDS surfactants were added to one box and 90 CTAB surfactants were added to the other box. After energy minimization and 60 ns *NVT* ensemble simulation, we obtained two kinds of oil droplets adsorbed by SDS and CTAB molecules. The dynamic formation process of the two types of oil droplet models is shown in Figure 1a.

The next step was to construct the system model for the demulsification of oil droplets under an electric field. It was worth noting that by comparing the adsorption process and adsorption results of surfactants on the oil droplet surface, we found that the adsorption capacity of the SDS surfactant on the oil droplet surface was 70, which was smaller than that of CTAB on the oil droplet surface. Therefore, in order to ensure that the demulsification process of oil droplets was not affected by the number of surfactants, the oil droplet model of adsorbed SDS and the oil droplet model of adsorbed CTAB used for demulsification contained the same number of surfactants and both were 70. Subsequently, we constructed system models for demulsification under the action of an electric field using the two types of emulsified oil droplet models mentioned above. The first simulation system was to place two oil droplet models adsorbing CTAB along the *z* axis in the center of a 15 × 15 × 50 nm^3 simulation box, to set the edge distance of the two oil droplets to 9 nm, and to add 76 Cl^- to balance the system charge. Finally, water molecules were randomly added. In the second simulation system, the two oil droplet models adsorbing SDS were placed in the center of a 15 × 15 × 50 nm^3 simulation box along the *z* axis, the edge distance of the two oil droplets was also set at 9 nm, and 204 Na^+ was added to balance the system charge. Finally, water molecules were added. The initial models of the two emulsion systems under an electric field are shown in Figure 1b.

3. RESULTS AND DISCUSSION

3.1. Formation Process and Structures of the Oil Droplets Adsorbed by Surfactants. First, the absorption process and the final structure models of oil droplets absorbed by SDS and CTAB molecules were compared. We extracted the system models of the *NVT* ensemble process at different times, as shown in Figure 2a. It was found that both SDS and CTAB surfactants would adsorb from the aqueous solution to the surface of oil droplets with the increase of simulation time, and a small part of the surfactants would self-aggregate and ultimately exist in the form of micelles. At the same time, we magnified the surfactant aggregates in the aqueous solutions of the two systems and found that the amount of surfactant contained in the two aggregates was different. In order to facilitate a comparison of the quantities of SDS and CTAB in aggregates, S and N atoms were represented as spheres. It was evident that there were more surfactants in the SDS aggregates. This also indicated that when SDS and CTAB are present in the aqueous solution, CTAB is more likely to adsorb on the surface of oil droplets. To verify this conclusion, we calculated the energy potential of interaction between surfactants and oil droplets during the interaction process. Figure 2b,c shows that the van der Waals interaction potential energy and the

https://doi.org/10.1021/acsomega.4c05623
ACS Omega 2024, 9, 48232−48245

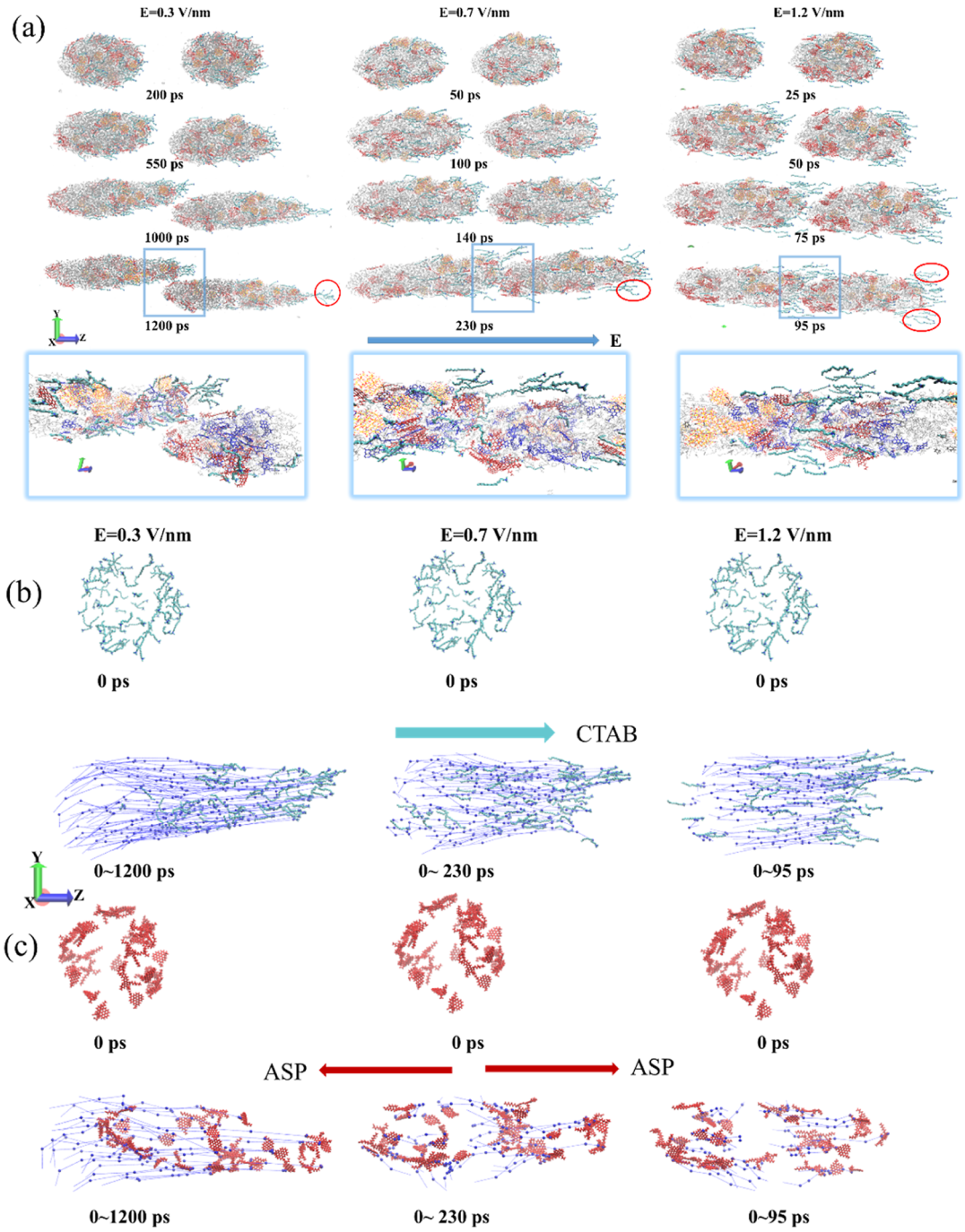

Figure 4. (a) Moving snapshots of the oil droplets absorbed by CTAB molecules under different electric field strengths. (b) Motion trajectory of CTAB molecules under different electric field strengths. (c) Motion trajectory of asphaltene molecules under different electric field strengths. Cyan stick models represent CTAB molecules, gray lines represent light oil molecules, red stick models are asphaltene molecules, blue stick models are resin molecules, and linear models are SiO_2 nanoparticles.

electrostatic interaction potential energy between CTAB molecules and oil droplets were both smaller than the interaction potential energy between SDS molecules and oil droplets, as well as influenced by negatively charged molecules on the surface of the oil droplets, and the electrostatic interaction potential energy between SDS molecules and oil droplets was positive. Through the interaction potential energy comparison, it is proved that CTAB molecules were more easily adsorbed on the surface of oil droplets.

We extracted two types of oil droplet models and labeled different regions of the oil droplet surface obtained from *NVT* ensemble simulation with different colors. From Figure 3a,b, we obtained that CTAB molecules were evenly distributed on the surface of oil droplets. However, SDS molecules appeared to be concentrated in parts of the oil droplet. Then, we extracted the adsorption conformations of CTAB and SDS on the oil droplet surface and found that CTAB irregularly adsorbed near asphaltene molecules, while SDS inserted between asphaltene molecules. In addition, we discovered that a small number of SDS molecules self-aggregated on the surface of the oil droplets. Moreover, in order to understand the differences in the interactions between the two types of

https://doi.org/10.1021/acsomega.4c05623
ACS Omega 2024, 9, 48232−48245

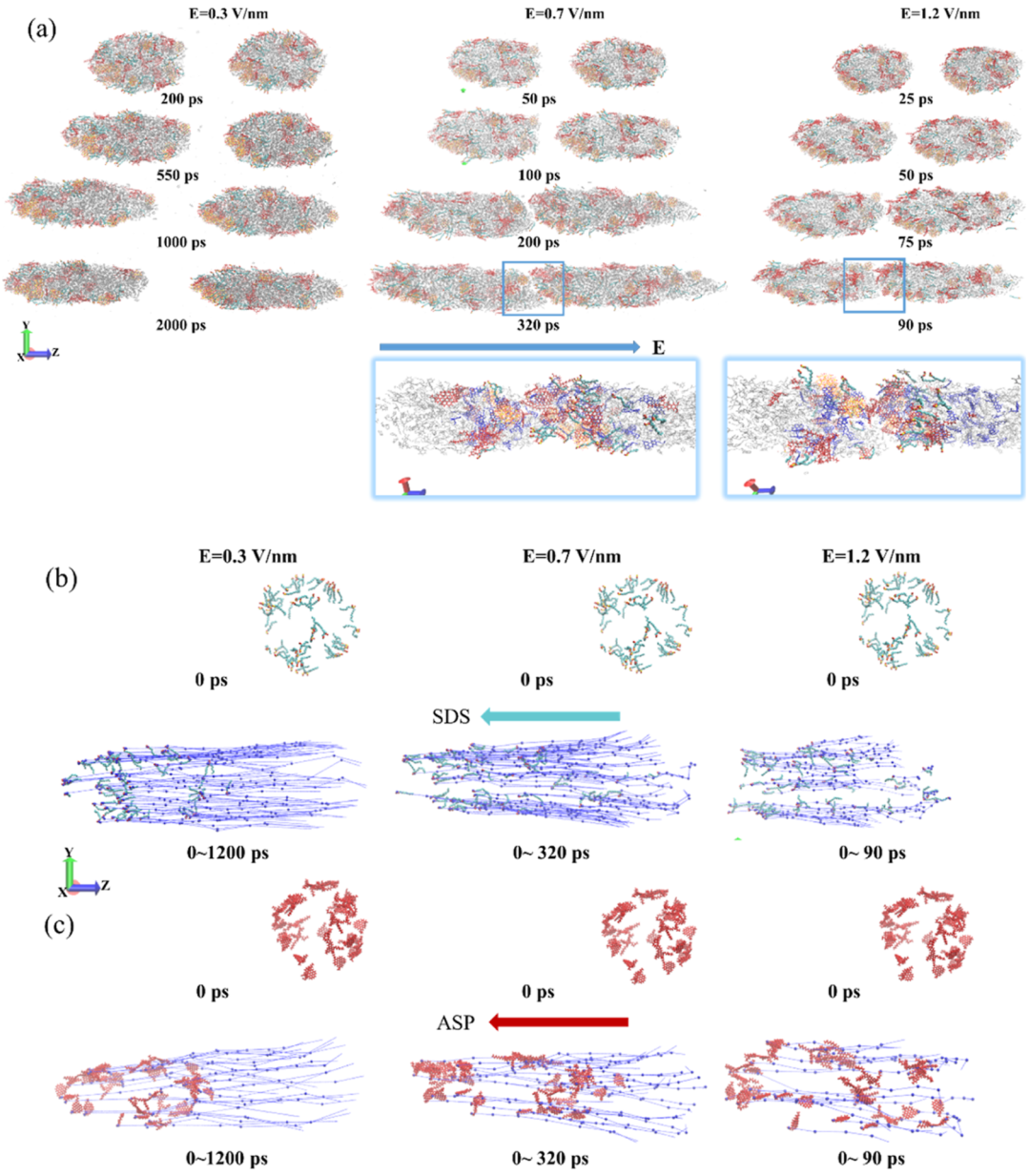

Figure 5. (a) Moving snapshots of the oil droplets absorbed by SDS molecules under different electric field strengths. (b) Motion trajectory of SDS molecules under different electric field strengths. (c) Motion trajectory of asphaltene molecules under different electric field strengths. Cyan stick models represent SDS molecules, gray lines represent light oil molecules, red stick models were asphaltene molecules, blue stick models were resin molecules, and linear models were SiO_2 nanoparticles.

surfactants and oil components, we analyzed the radial distribution function (RDF) between surfactants and oil molecules during the *NVT* ensemble equilibrium stage. To a certain extent, the RDF can reflect the interaction between the reference atom/molecule and the counted atom/molecule.[50] Figure 3c shows the RDF between CTAB molecules and SiO_2 nanoparticles, asphaltene molecules, and resin molecules. Figure 3d shows the RDF between SDS molecules and SiO_2 nanoparticles, asphaltene molecules, and resin molecules. We noted that the interaction between CTAB and SiO_2 nanoparticles, asphaltene molecules, and resin molecules was stronger than that between SDS surfactants. The difference in interaction strength between the surfactant and asphaltene molecules was the largest. We believed that the electrostatic interaction between positively charged CTAB molecules and negatively charged asphaltene molecules enhanced the interaction intensity between CTAB molecules and asphaltene molecules. At the same time, compared with the random adsorption of CTAB around asphaltene, the unique aggregation mode of SDS molecules on the surface of oil droplets made part of SDS molecules gather between asphaltene molecules and part of SDS molecules kept away from asphaltene molecules, thus reducing the interaction strength between SDS and asphaltene molecules. Therefore, the interaction between CTAB molecules and oil droplet components was stronger than that of SDS molecules.

3.2. Analysis of Oil Droplet Behavior under an Electric Field. Figure 4a shows the simulation snapshots of the oil droplets adsorbed by CTAB molecules at different times under different electric field strengths. First, we found that the oil droplets changed from a circular shape to an elliptical shape under the action of the electric field. Second, the oil droplet

https://doi.org/10.1021/acsomega.4c05623
ACS Omega 2024, 9, 48232−48245

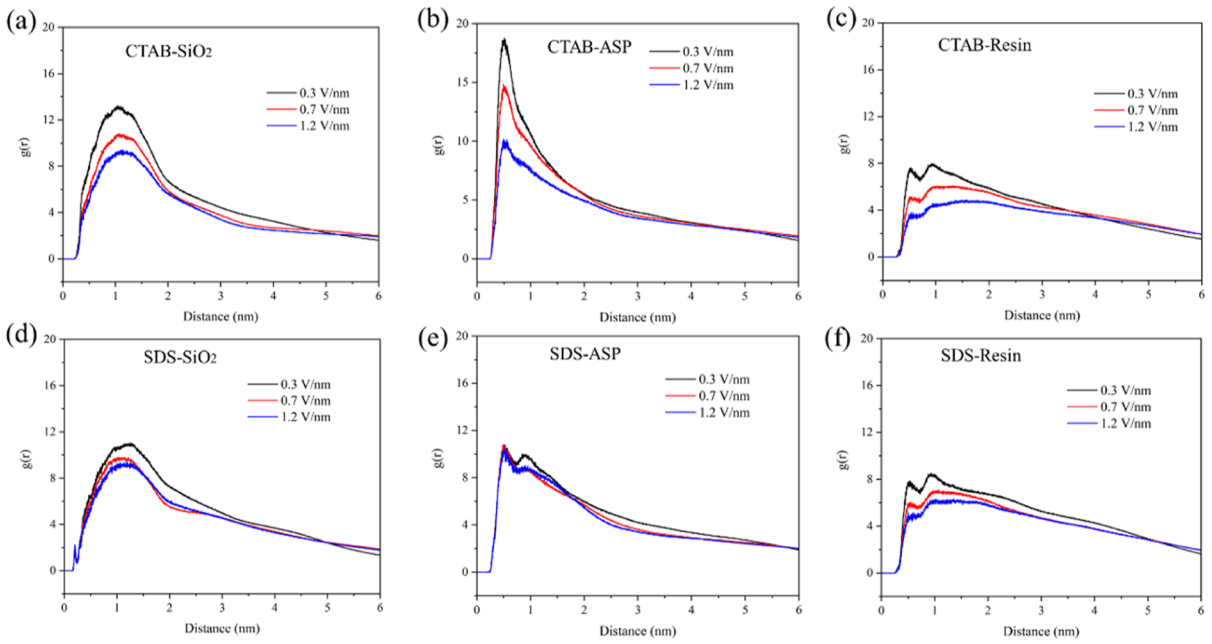

Figure 6. RDF between the CTAB surfactant and some molecules in oil droplets (a−c). RDF between the SDS surfactant and some molecules in oil droplets (d−f).

moved in the direction of the applied electric field, and the uniformly distributed CTAB molecules on the surface of the oil droplet quickly transferred to the head position of the oil droplet movement. It could be seen that the positively charged CTAB played a pulling effect on the oil droplet and drove the oil droplet to move in the direction of the applied electric field. Meanwhile, with the increase of electric field strength, the time required for oil droplet coalescence decreased. In addition, we discovered that CTAB molecules were affected by the electric field, and part of the CTAB molecules left the oil droplet, entered the water phase, and moved parallel to the electric field direction, as shown in the red circle in Figure 4a. Finally, we enlarged the interface where the two oil droplets just started to contact, as shown in Figure 4a. It is worth mentioning that after the CTAB molecules between adjacent oil droplets were freed from the oil droplet bondage, the oil-phase molecules were exposed to the water phase, and it was easy to coalesce with the oil-phase molecules of adjacent oil droplets.

In order to observe the migration of charged molecules in oil droplets under the electric field more intuitively, we extracted the motion trajectory of CTAB and asphaltene molecules of one oil droplet, as shown in Figure 4b,c, where the blue dots represent the molecular movement position over time. It was not difficult to see that the CTAB molecules moved in the direction of the applied electric field. The negatively charged asphaltene molecules near the head of the oil droplet were pulled by the CTAB molecules, which were consistent with the direction of the applied electric field. The asphaltene molecules far from the head of the oil droplet were greatly affected by the electric field, and their migration direction was opposite to that of CTAB molecules, which was to move in the opposite direction of the applied electric field. This simulated phenomenon is similar to the experimental phenomenon and conclusion of Wang et al.;[51] that is, the negatively charged oil droplets started to migrate toward the anode under a DC electric field. The application of a DC electric field destabilized the charge structure on the surface of the oil droplet, causing an unbalanced charge distribution on the surface of the oil droplet and resulting in the directional migration of the oil droplet.

Figure 5a shows the simulation snapshots of the oil droplets adsorbed by SDS molecules at different times under different electric field strengths. Similar to the above phenomenon, the oil droplets undergone deformation and changed from a circular shape to an elliptical shape under the influence of an electric field. The motion trajectories of SDS and asphaltene molecules in the oil droplet are shown in Figure 5b,c. It was obvious that the movement direction of SDS and asphaltene molecules was opposite to the direction of the electric field. This is consistent with the results obtained by Wang et al. and Qi et al.[36,37] in simulating the movement behavior of the oil droplets adsorbed by SDS molecules in an electric field. Therefore, the negatively charged SDS and asphaltene molecules jointly pulled the oil droplet to move in the opposite direction of the electric field. In addition, it was worth noting that the oil droplets adsorbed by SDS molecules did not come into coalescence under low electric field strength (0.3 V/nm). Compared with the oil droplets adsorbed by CTAB molecules, under the 0.7 V/nm electric field strength, the coalescence time between two oil droplets absorbed by SDS molecules was longer, while, under the 1.2 V/nm electric field strength, the coalescence time of the two types of oil droplets was similar. Therefore, compared to the oil droplets adsorbed by CTAB molecules, the low electric field strength was not conducive to the coalescence of the oil droplets absorbed by SDS molecules. Furthermore, we locally magnified the interface between the two oil droplets in Figure 5a and found that compared to CTAB molecules, SDS molecules did not quickly transfer to the head of the oil droplet and freed from oil droplet bondage under the action of the electric field. Instead, they migrated together with asphaltene molecules in the opposite direction of the electric field.

Based on the behavioral difference of SDS, CTAB, and asphaltene molecules in the oil droplet under the action of the

https://doi.org/10.1021/acsomega.4c05623
ACS Omega 2024, 9, 48232−48245

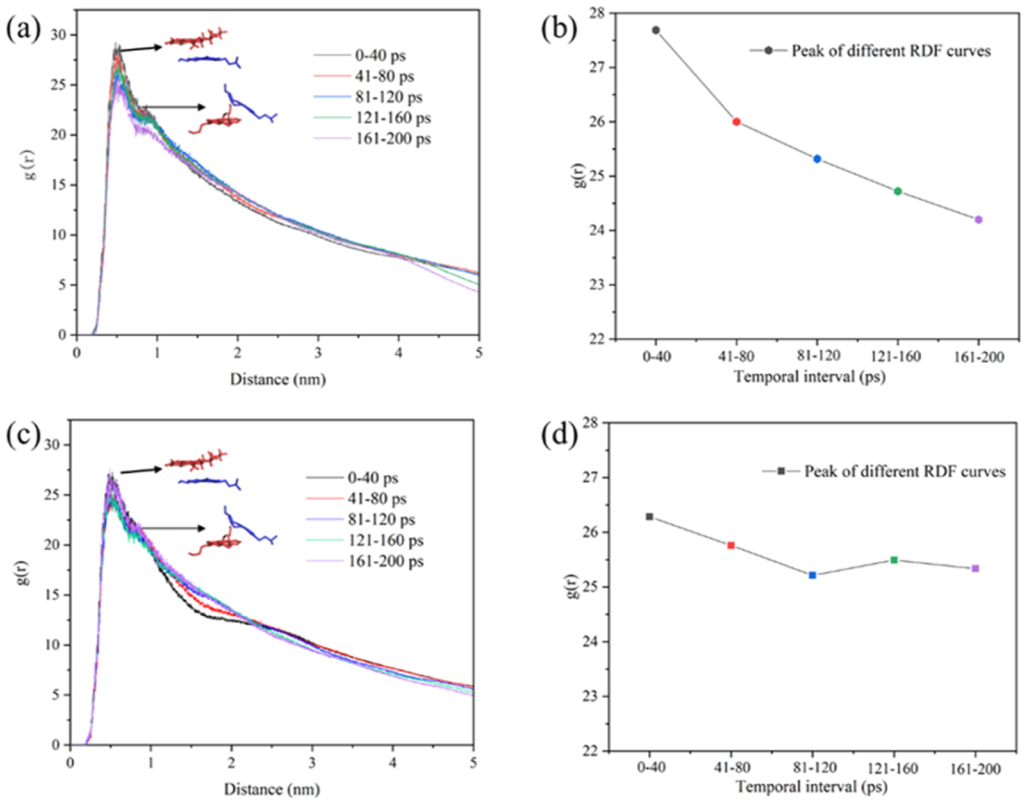

Figure 7. RDF between the asphaltene and resin molecules of the two types of oil droplets before coalescence under an electric field strength of 0.7 V/nm. (a,b) Oil droplet absorbed by CTAB molecules and (c,d) oil droplet absorbed by SDS molecules.

electric field, we calculated the RDF between SDS and some component molecules of the oil droplet, as well as CTAB and some component molecules of the oil droplet. The statistical results are shown in Figure 6. As shown in Figure 6—c, the greater the applied electric field strength, the weaker the interaction between CTAB molecules and the components of the oil droplet. We thought that the movement rate of CTAB molecules increased under higher electric field strength, which weakened the interaction between CTAB molecules and the molecules of the oil droplet. Figure 6—f shows the RDF between SDS and some component molecules of the oil droplet under different electric field strengths. Similarly, the interaction between SDS molecules and SiO_2 nanoparticles and resin molecules in oil droplets decreased with the increase in electric field strength. However, the RDF curves between SDS and asphaltene molecules were similar under different electric field strengths. In other words, there was no significant change in the interaction between SDS and asphaltene molecules. This was attributed to the fact that SDS molecules, which aggregated between asphaltene molecules, moved in the same direction as asphaltene molecules under an electric field. This also explained why the SDS molecules on the surface of the oil droplet did not quickly transfer to the moving head of the oil droplet and free from oil droplets in the electric field.

In addition, taking the 0.7 V/nm electric field strength applied to each system as an example, the mean square displacement (MSD) of surfactants, asphaltenes, and SiO_2 nanoparticles in oil droplets during the electric field application stage (Figure S2), as well as the potential energy changes of interaction between SiO_2 nanoparticles and asphaltenes and between SiO_2 nanoparticles and surfactants, was analyzed (Figure S3). It is found that the motion of SiO_2 nanoparticles in the electric field is mainly affected by asphaltene molecules.

3.3. Reasons for the Behavioral Difference of the Two Types of Oil Droplets under an Electric Field. The oil droplets moved in a directional direction under the action of an electric field and gradually deformed. Meanwhile, the density of the droplets gradually decreased during this process. In the oil droplet, the aromatic region of asphaltene molecules easily forms face-to-face and face-to-edge stacking structures with the resin molecules with the same aromatic region. With the deformation of the oil droplet, the stacking structures are bound to change. To verify this process, we analyzed the RDF between the asphaltene and resin molecules of the two types of oil droplets at different time periods under the action of an electric field strength of 0.7 V/nm (Figure 7). From Figure 7a,c, we found that the interaction strength between asphaltene and resin in the two types of oil droplets decreased with the extension of time of applying the electric field, and the change of oil droplets containing CTAB was more obvious. This showed that the stacking structures of the oil droplets changed and gradually weakened under the action of the electric field. We calculated the peak value of RDF between asphaltene and resin in different time periods and found that the peak value of RDF between the asphaltene and resin molecules of oil droplets containing CTAB decreased faster than that of oil droplets containing SDS, as shown in Figure 7b,d. This indicated that the oil droplet containing CTAB became loose faster under the electric field than the oil droplet containing SDS. At the same time, the stacking structure changes of oil droplets under the electric field strength of 0.3 and 1.2 V/nm were analyzed in the same way, as shown in Figure S4. We discovered that under the action of an electric field strength of

https://doi.org/10.1021/acsomega.4c05623
ACS Omega 2024, 9, 48232—48245

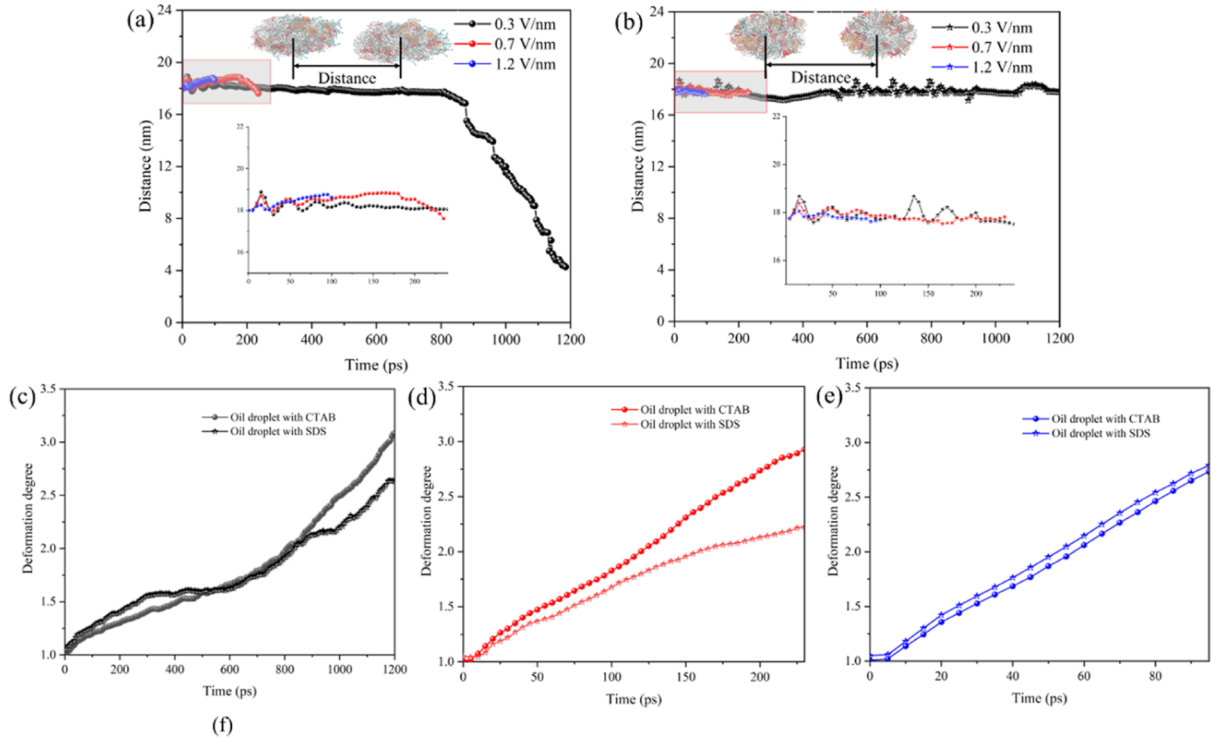

Figure 8. Central distance of the two oil droplets and the average degree of deformation of the two oil droplets under different electric field strengths. (a) Central distance of the two oil droplets absorbed by CTAB molecules. (b) Central distance of the two oil droplets absorbed by SDS molecules. (c) Degree of deformation of the two oil droplets under an electric field of 0.3 V/nm. (d) Degree of deformation of the two oil droplets under an electric field of 0.7 V/nm. (e) Degree of deformation of the two oil droplets under an electric field of 1.2 V/nm.

0.3 V/nm, the stacking structures of the oil droplet containing CTAB loosened faster than that of the oil droplet containing SDS. However, when an electric field strength of 1.2 V/nm was applied in O/W emulsion systems, the two types of oil droplets had similar structural loose speed. This was consistent with the statistical results of coalescence time of the two types of oil droplets under different electric field strengths. We thought this was due to the fact that the positively charged CTAB molecules and the negatively charged asphaltene molecules move in opposite directions, causing the oil droplets to loose faster at low electric field strengths compared to the oil droplets containing SDS.

In order to further explain the difference in the coalescence behavior of the two types of oil droplets in an electric field, we measured the central distance of the two types of oil droplets before coalescence under an electric field. Figure 8a shows the central distance of the oil droplets adsorbed by CTAB molecules under the action of electric fields with different strengths, and Figure 8b shows the central distance of the oil droplets adsorbed by SDS molecules under the action of electric fields with different strengths. We discovered that the central distance of the two types of oil droplets was always around 18 nm. From this, it could be seen that the two oil droplets moved almost at the same speed in the z-direction under the action of an electric field. However, it should be noted that under the 0.3 V/nm electric field strength, the central distance between the two CTAB-absorbed oil droplets gradually decreases after 700 ns, which was consistent with the deformation behavior of CTAB-emulsified oil under the 0.3 V/nm electric field strength in Figure 4a. We found that the head of the oil droplet was close to the tail of the other oil droplet under the electric field, but due to the spatial hindrance of the front oil droplet, the moving direction of the rear oil droplet was shifted under the guidance of CTAB, and as a result, the central distance of oil droplets gradually decreased. In addition, we took the electric field strength of 0.7 V/nm applied to the systems as an example to analyze the change of the central distance of oil droplets in the systems and the change of the deformation length of oil droplets under the action of electric fields, as shown in Figure S5. The results show that the central distance between oil droplets is always about 18 nm, and the deformation length of oil droplets increases with time. In other words, when the adjacent oil droplets move under the action of the electric field, the length of the oil droplets increases along the direction of movement, and at some moment, the moving tail of the oil droplets in the front and the moving head of the oil droplets in the back coalesce; that is, the oil droplets of the systems migrated and coalesced under the action of the electric field.

Then, we analyzed the deformation degree of oil droplets under the action of an electric field. The coalescence of oil droplets under the action of an electric field is realized on the basis of the deformation of oil droplets. Statistics on the deformation degree of the two types of oil droplets in the electric field can further explain the reason for the difference in the coalescence time of the two types of oil droplets. The deformation degree D is calculated by the formula

$$D = \frac{d_1}{d_2}$$

where d_1 represents the length change of oil droplets stretched under the electric field, similar to the elliptical long axis, and d_2 represents the width change of oil droplets perpendicular to the electric field direction after being stretched, similar to the

https://doi.org/10.1021/acsomega.4c05623
ACS Omega 2024, 9, 48232−48245

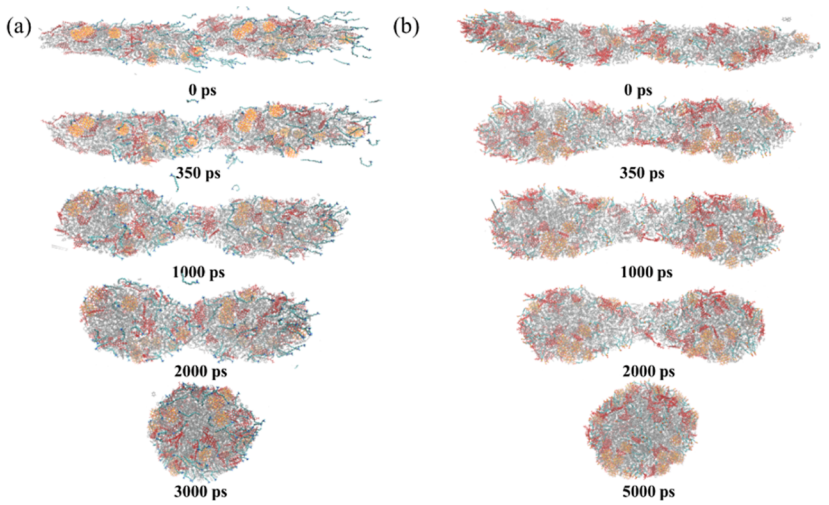

Figure 9. Behavior snapshots of the two oil droplets in the O/W emulsion of removing the electric field. (a) Oil droplets absorbed by CTAB molecules. (b) Oil droplets absorbed by SDS molecules.

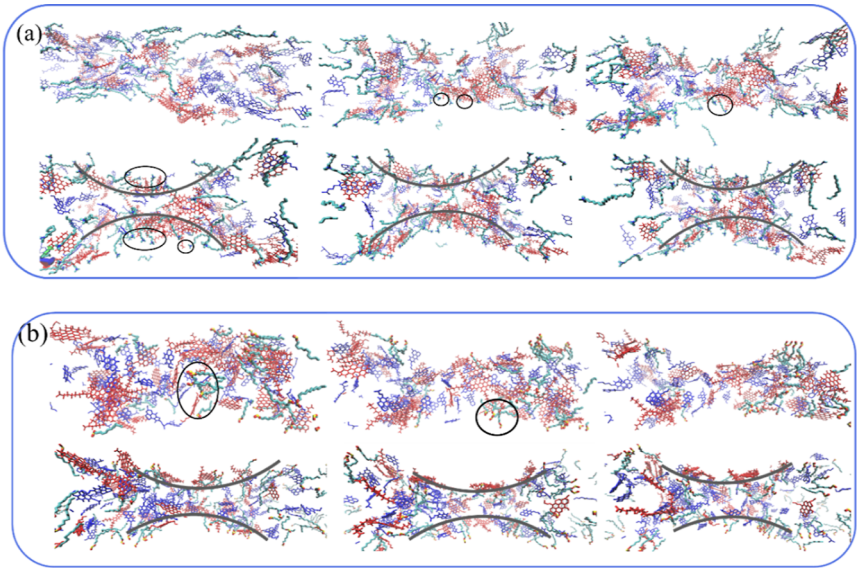

Figure 10. Enlarged views of the junction of the oil droplets at different times after removing the electric field. (a) Oil droplets absorbed by CTAB molecules. (b) Oil droplets absorbed by SDS molecules.

elliptical short axis. The greater the deformation degree of the oil droplet, the longer the stretching length of the oil droplet along the *z*-axis and the smaller the width of the oil droplet perpendicular to the *z*-axis. Meanwhile, the length of the oil droplets in the *z*-direction is larger, which is more conducive to coalescing between the two oil droplets. From Figure 8c,d, it could be seen that the deformation degree of the two types of oil droplets was significantly different under the action of electric fields (0.3 and 0.7 V/nm). The deformation degree of the oil droplet absorbed by CTAB molecules during the same time was higher than that of the oil droplet absorbed by SDS molecules. It could also be said that the stretching length of CTAB-adsorbed oil droplets in the *z*-direction changed faster under the action of electric fields, so the coalescence time required under the electric field of oil droplets absorbed by CTAB molecules was shorter than that required under the electric field of oil droplets absorbed by SDS molecules. Under the electric field strength of 1.2 V/nm, the deformation degree of the two types of oil droplets was similar, as shown in Figure 8e. This indicates that the deformation length of the two types of oil droplets was similar, and the coalescence time required of oil droplets was similar, which was consistent with the snapshot statistical results of the coalescence time of the two types of oil droplets in Figures 4a and 5a. Figure 8c–e proved that the deformation degree of the oil droplets absorbed by CTAB molecules than that of the oil droplets adsorbed by SDS molecules at low electric field strength, which was more conducive to coalesce between oil droplets. It also further explained the reason for the difference in the behavioral changes and coalescence time of the two types of oil droplets under low electric field strength.

3.4. Change of the Behavior of Coalesced Oil Droplets after Removing the Electric Field. The purpose of demulsification of the O/W emulsions under an electric field is to aggregate dispersed oil droplets and achieve oil–water separation. Some researchers have found that the pulsed-DC electric field can be used to achieve higher coalescence efficiency.[34,52] Therefore, we chose the conformations of the

https://doi.org/10.1021/acsomega.4c05623
ACS Omega 2024, 9, 48232–48245

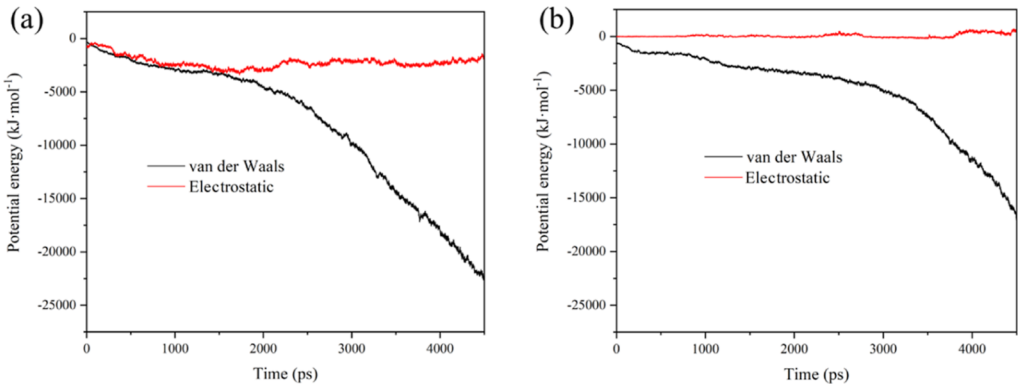

Figure 11. (a) Interaction of potential energy during demulsification of the oil droplets absorbed by CTAB molecules and (b) interaction of potential energy during demulsification of the oil droplets absorbed by SDS molecules.

moment when the oil droplets in the two systems began to coalesce under the action of 0.7 V/nm electric field strength as the initial model to simulate the behavioral changes of the oil droplets after removal of the electric field (Figure 9a,b). We found that oil droplets absorbed by CTAB molecules continue to aggregate after coalescing, even in the absence of an electric field. During the demulsification process of the two oil droplets, the oil droplets gradually changed from an elliptical shape to a spherical shape, forming a dumbbell shape and eventually melting into a whole. In addition, during the demulsification process of the two oil droplets absorbed by SDS molecules, the oil droplets also gradually changed from an elliptical shape to a spherical shape, forming a dumbbell shape and eventually melting into a whole. However, it should be noted that the demulsification process of the oil droplets absorbed by SDS molecules took longer than that of the oil droplets absorbed by SDS molecules.

In order to explore the behavioral differences during the demulsification process of the two types of oil droplets, we extracted structural snapshots of the interface at different times during the demulsification of oil droplets, as shown in Figure 10. From Figure 10a, it was found that the headgroup of CTAB molecules at the oil droplet interface formed binding conformations with the negatively charged asphaltene molecules in the adjacent oil droplet, which enhanced the interaction between the two oil droplets. With the increase of simulation time, the asphaltene molecules and CTAB molecules of the oil droplet junction penetrated into the water phase, and a channel for other components of the oil droplet was formed to coalesce. For the oil droplets adsorbed by SDS molecules, as shown in Figure 10b, after removing the electric field, the SDS molecules at the oil droplet interface gradually penetrated into the water phase. The junction of the oil droplets formed a bridge structure made of asphaltene and resin molecules. With the extension of the simulation time, the hydrophilic asphaltene molecules migrated to the surface of the oil droplet junction, providing a channel for other oil molecules to coalesce.

Considering the different interaction relationships between CTAB molecules and SDS molecules with the components of oil droplets during the demulsification process, we calculated the interaction potential energy during the demulsification process of oil droplets in the two systems. From Figure 11a,b, it was found that the van der Waals interaction potential energy significantly decreased during the demulsification process between oil droplets adsorbed by CTAB molecules; meanwhile, the electrostatic interaction potential energy between oil droplets decreased. This was attributed to the electrostatic attraction between CTAB molecules and asphaltene molecules. Compared to the oil droplets adsorbed by CTAB molecules, during the demulsification process of the two oil droplets adsorbed by SDS molecules, the van der Waals interaction potential energy significantly decreases, while the electrostatic interaction potential energy did not change significantly. In other words, the two oil droplets containing SDS molecules were mainly demulsified by the van der Waals interaction between oil droplets, while the oil droplets containing CTAB molecules were demulsified by the electrostatic attraction between CTAB and asphaltene in addition to the van der Waals interaction between oil droplets. At the same time, it can be determined that the main force of the oil droplet demulsification process is van der Waals.

Based on the above analysis, it can be concluded that the oil droplets adsorbed by CTAB molecules are more likely to coalesce under a low electric field strength than the oil droplets absorbed by SDS molecules. At the same time, when the electric field of the two oil droplets was removed, the interaction between the CTAB molecule and asphaltene molecule could enhance the demulsification speed of oil droplets. To further determine that it is not accidental for the oil droplets absorbed by CTAB molecules to coalesce more easily under low electric fields, we measured the time required for oil droplet coalescence between the two types of oil droplets under multiple electric field strengths. The statistical results are shown in Figure 12. It was noted that oil droplets containing CTAB molecules could coalesce when the electric field strength was above 0.3 V/nm, while oil droplets containing SDS molecules could coalesce only when the electric field strength was above 0.5 V/nm. However, after an electric field strength greater than 0.8 V/nm, the difference in coalescence time between the two types of oil droplets under the electric field gradually decreased. It could be seen that under low electric field strength, the oil droplets with CTAB molecules have a better demulsification effect than the oil droplets with SDS molecules.

4. CONCLUSIONS

In this work, MD methods were used to study the behavioral changes and demulsification mechanism of oil droplets adsorbed by different surfactants under the action of an electric field. First, the adsorption differences and adsorption structures of CTAB and SDS surfactants on the surfaces of oil

https://doi.org/10.1021/acsomega.4c05623
ACS Omega 2024, 9, 48232−48245

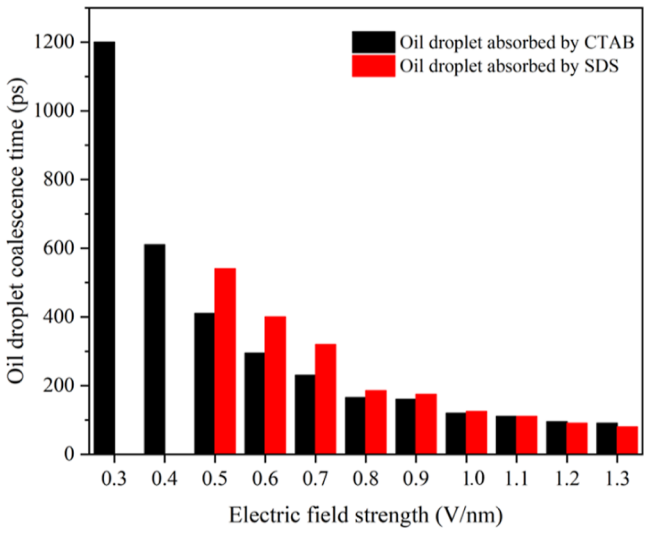

Figure 12. Coalescence time required for the two types of oil droplets under different electric field strengths.

droplets were compared. According to the potential energy analysis of the interaction between surfactants and oil droplets, it was found that CTAB molecules were more easily adsorbed on the surface of oil droplets than SDS molecules, and CTAB molecules were evenly distributed on the surface of oil droplets.

In the process of exploring the effects of electric field intensity and surfactant type on the demulsification behavior of oil droplets, it was found that after the electric field was applied to the O/W emulsion systems, SiO_2 nanoparticles and oil molecules in the oil droplets moved directionally under the traction of charged molecules, and the coalescence time between oil droplets decreased with the increase of electric field intensity. Compared with the oil droplets adsorbed by SDS molecules, the motion direction of CTAB molecules and asphaltene molecules in the oil droplets adsorbed by CTAB molecules was opposite under the action of the electric field, resulting in oil droplets adsorbed by CTAB molecules in faster deformation and loose speed under low electric field intensity, which accelerated the coalescence between oil droplets.

Finally, at the stage of stopping the output electric field, the coalesced oil droplets could spontaneously coalesce into a whole to complete oil droplet demulsification. During the demulsification process, at the interface of the two oil droplets adsorbed by CTAB molecules, electrostatic attraction was generated between CTAB molecules and asphaltene molecules in adjacent oil droplets, which accelerated the interaction between oil droplets and promoted the demulsification of oil droplets. For the oil droplets adsorbed by SDS molecules, the asphaltene and resin molecules between the oil droplets first established a bridge structure for the two oil droplets to demulsify; however, the potential energy of the electrostatic interaction between the oil droplets did not change, and the demulsification process mainly depended on the van der Waals force between the oil droplets.

■ ASSOCIATED CONTENT

Supporting Information

The Supporting Information is available free of charge at https://pubs.acs.org/doi/10.1021/acsomega.4c05623.

Asphaltene and resin molecules used in the simulations; MSD of surfactants, asphaltenes, and SiO_2 nanoparticles; potential energy changes of the interaction between SiO_2 nanoparticles and asphaltenes and between SiO_2 nanoparticles and surfactants; RDF between the asphaltene and resin molecules of two types of oil droplets before coalescence; and change of central distance of oil droplets and deformation length of oil droplets under the action of electric field (PDF)

■ AUTHOR INFORMATION

Corresponding Authors

Shasha Liu − *School of Chemistry and Chemical Engineering, Qilu Normal University, Jinan 250000, PR China; School of Chemistry and Chemical Engineering, Shandong University, Jinan 250000, PR China*; Email: lshasha@qlnu.edu.cn

Shiling Yuan − *School of Chemistry and Chemical Engineering, Shandong University, Jinan 250000, PR China*; orcid.org/0000-0002-4073-9470; Email: shilingyuan@sdu.edu.cn

Authors

Heng Zhang − *School of Chemistry and Chemical Engineering, Shandong University, Jinan 250000, PR China*; orcid.org/0009-0008-3680-5480

Shideng Yuan − *School of Chemistry and Chemical Engineering, Shandong University, Jinan 250000, PR China*

Complete contact information is available at: https://pubs.acs.org/10.1021/acsomega.4c05623

Notes

The authors declare no competing financial interest.

■ ACKNOWLEDGMENTS

We gratefully appreciate the financial support from the Natural Science Foundation of Shandong Province (No. ZR2021MB040).

■ REFERENCES

(1) Binks, B. P.; Rodrigues, J. A. Enhanced stabilization of emulsions due to surfactant-induced nanoparticle flocculation. *Langmuir* **2007**, *23* (14), 7436−7439.

(2) Hannisdal, A.; Ese, M. H.; Hemmingsen, P. V.; Sjöblom, J. Particle-stabilized emulsions: Effect of heavy crude oil components pre-adsorbed onto stabilizing solids. *Colloids Surf., A* **2006**, *276* (1−3), 45−58.

(3) Sullivan, A. P.; Kilpatrick, P. K. The Effects of Inorganic Solid Particles on Water and Crude Oil Emulsion Stability. *Ind. Eng. Chem. Res.* **2002**, *41* (14), 3389−3404.

(4) Levine, S.; Sanford, E. Stabilisation of emulsion droplets by fine powders. *Can. J. Chem. Eng.* **1985**, *63*, 258−268.

(5) Pereira, M. L. d. O.; Maia, K. C. B.; Silva, W. C.; Leite, A. C.; Francisco, A. D. d. S.; Vasconcelos, T. L.; Nascimento, R. S. V.; Grasseschi, D. Fe3O4 Nanoparticles as Surfactant Carriers for Enhanced Oil Recovery and Scale Prevention. *ACS Appl. Nano Mater.* **2020**, 3 (6), 5762−5772.

(6) Al-Azani, K.; Abu-Khamsin, S.; Al-Abdrabalnabi, R.; Kamal, M. S.; Patil, S.; Zhou, X.; Hussain, S. M. S.; Al Shalabi, E. Oil Recovery Performance by Surfactant Flooding: A Perspective on Multiscale Evaluation Methods. *Energy Fuels* **2022**, *36* (22), 13451−13478.

(7) Zolfaghari, R.; Fakhru'l-Razi, A.; Abdullah, L. C.; Elnashaie, S. S. E. H.; Pendashteh, A. Demulsification techniques of water-in-oil and oil-in-water emulsions in petroleum industry. *Sep. Purif. Technol.* **2016**, *170*, 377−407.

(8) Opawale, F. O.; Burgess, D. J. Influence of Interfacial Properties of Lipophilic Surfactants on Water-in-Oil Emulsion Stability. *J. Colloid Interface Sci.* **1998**, *197* (1), 142−150.
(9) Guha, I. F.; Varanasi, K. K. Low-Voltage Surface Electrocoalescence Enabled by High-K Dielectrics and Surfactant Bilayers for Oil-Water Separation. *ACS Appl. Mater. Interfaces* **2019**, *11* (38), 34812−34818.
(10) Alvarado, V.; Wang, X.; Moradi, M. Stability Proxies for Water-in-Oil Emulsions and Implications in Aqueous-based Enhanced Oil Recovery. *Energies* **2011**, *4* (7), 1058−1086.
(11) Yan, L. T.; Schoberth, H. G.; Böker, A. Lamellar microstructure and dynamic behavior of diblock copolymer/nanoparticle composites under electric fields. *Soft Matter* **2010**, *6* (23), 5956−5964.
(12) Vivacqua, V.; Mhatre, S.; Ghadiri, M.; Abdullah, A. M.; Hassanpour, A.; Al-Marri, M. J.; Azzopardi, B.; Hewakandamby, B.; Kermani, B. Electrocoalescence of water drop trains in oil under constant and pulsatile electric fields. *Chem. Eng. Res. Des.* **2015**, *104*, 658−668.
(13) Eow, J. S.; Ghadiri, M.; Sharif, A. O.; Williams, T. J. Electrostatic enhancement of coalescence of water droplets in oil: a review of the current understanding. *Chem. Eng. J.* **2001**, *84* (3), 173−192.
(14) Eow, J. S.; Ghadiri, M. Electrostatic enhancement of coalescence of water droplets in oil: a review of the technology. *Chem. Eng. J.* **2002**, *85* (2−3), 357−368.
(15) Mohammadian, E.; Taju Ariffin, T. S.; Azdarpour, A.; Hamidi, H.; Yusof, S.; Sabet, M.; Yahya, E. Demulsification of Light Malaysian Crude Oil Emulsions Using an Electric Field Method. *Ind. Eng. Chem. Res.* **2018**, *57* (39), 13247−13256.
(16) Mhatre, S.; Simon, S.; Sjöblom, J.; Xu, Z. Demulsifier assisted film thinning and coalescence in crude oil emulsions under DC electric fields. *Chem. Eng. Res. Des.* **2018**, *134*, 117−129.
(17) Muto, A.; Hiraguchi, Y.; Kinugawa, K.; Matsumoto, T.; Mizoguchi, Y.; Tokumoto, H. Effects of organic solvent and ionic strength on continuous demulsification using an alternating electric field. *Colloids Surf., A* **2016**, *506*, 228−233.
(18) Zagnoni, M.; Le Lain, G.; Cooper, J. M. Electrocoalescence Mechanisms of Microdroplets Using Localized Electric Fields in Microfluidic Channels. *Langmuir* **2010**, *26* (18), 14443−14449.
(19) Gong, H.; Yu, B.; Peng, Y.; Dai, F. Promoting coalescence of droplets in oil subjected to pulsed electric fields: changing and matching optimal electric field intensity and frequency for demulsification. *J. Dispersion Sci. Technol.* **2019**, *40*, 1236−1245.
(20) Ren, B.; Kang, Y. Aggregation of Oil Droplets and Demulsification Performance of Oil-in-water Emulsion in Bidirectional Pulsed Electric Field. *Sep. Purif. Technol.* **2019**, *211*, 958−965.
(21) Zhang, L.; He, L.; Ghadiri, M.; Hassanpour, A. Effect of surfactants on the deformation and break-up of an aqueous drop in oils under high electric field strengths. *J. Pet. Sci. Eng.* **2015**, *125*, 38−47.
(22) Yang, D.; Sun, Y.; He, L.; Luo, X.; Lü, Y.; Gao, Q. Partial coalescence of droplets at oil−water interface subjected to different electric waveforms: Effects of non-ionic surfactant on critical electric field strength. *Chem. Eng. Res. Des.* **2019**, *142*, 214−224.
(23) Mizoguchi, Y.; Muto, A. Demulsification of Oil-in-Water Emulsions by Application of an Electric Field: Relationship between Droplet Size Distribution and Demulsification Efficiency. *J. Chem. Eng. Jpn.* **2019**, *52* (10), 799−804.
(24) Li, L. J.; Cao, Q. Q.; Liu, H.; Qiao, X. Molecular dynamics study of electrocoalescence of pure water and salty nanodroplets. *J. Mol. Liq.* **2021**, *332*, 115895.
(25) Li, N.; Sun, Z. Q.; Sun, J. H.; Liu, W. C.; Wei, L. C.; Li, T.; Li, B.; Wang, Z. B. Deformation and breakup mechanism of water droplet in acidic crude oil emulsion under uniform electric field: A molecular dynamics study. *Colloids Surf., A* **2022**, *632*, 127746.
(26) Li, N.; Sun, Z. Q.; Liu, W. C.; Wei, L. C.; Li, B.; Qi, Z.; Wang, Z. B. Effect of electric field strength on deformation and breakup behaviors of droplet in oil phase: A molecular dynamics study. *J. Mol. Liq.* **2021**, *333*, 115995.
(27) He, X.; Zhang, B. X.; Wang, S. L.; Wang, Y. F.; Yang, Y. R.; Wang, X. D.; Lee, D. J. Electrocoalescence of two charged nanodroplets under different types of external electric fields. *J. Mol. Liq.* **2021**, *341*, 117417.
(28) Wang, Z. B.; Li, N.; Sun, Z. Q.; Wang, X. L.; Chen, Q.; Liu, W. C.; Qi, Z.; Wei, L. C.; Li, B. Molecular dynamics study of droplet electrocoalescence in the oil phase and the gas phase. *Sep. Purif. Technol.* **2021**, *278*, 119622.
(29) Li, N.; Pang, Y.; Sun, Z.; Sun, X.; Li, W.; Sun, Y.; Zhu, L.; Li, B.; Wang, Z.; Zeng, H. Unraveling Partial Coalescence Between Droplet and Oil−Water Interface in Water-in-Oil Emulsions under a Direct-Current Electric Field via Molecular Dynamics Simulation. *Langmuir* **2024**, *40* (11), 5992−6003.
(30) Li, N.; Pang, Y.; Sun, Z.; Li, W.; Sun, Y.; Sun, X.; Liu, Y.; Li, B.; Wang, Z.; Zeng, H. Effects of surfactants on droplet deformation and breakup in water-in-oil emulsions under DC electric field: A molecular dynamics study. *Fuel* **2024**, *358*, 130328.
(31) Wang, B.-B.; Wang, X.-D.; Yan, W.-M.; Wang, T.-H. Molecular Dynamics Simulations on Coalescence and Non-coalescence of Conducting Droplets. *Langmuir* **2015**, *31* (27), 7457−7462.
(32) Dong, H.; Liu, Y.; Zhou, Y.; Liu, T.; Li, M.; Yang, Z. Mechanism investigation of coalescence behaviors of conducting droplets by molecular dynamics simulations. *Colloids Surf., A* **2019**, *570*, 55−62.
(33) Li, B.; Dou, X.; Yu, K.; Li, N.; Zhang, W.; Xu, H.; Sun, Z.; Wang, Z.; Wang, J. Molecular dynamics simulations of nanoparticle-laden drop−interface electrocoalescence behaviors under direct and alternating current electric fields. *J. Mol. Liq.* **2021**, *344*, 117875.
(34) Wang, B.-B.; Wang, X.-D.; Wang, T.-H.; Lu, G.; Yan, W.-M. Electro-coalescence of two charged droplets under constant and pulsed DC electric fields. *Int. J. Heat Mass Transfer* **2016**, *98*, 10−16.
(35) Qi, Z.; Sun, Z.; Li, N.; Chen, Q.; Liu, W.; Li, W. J. Effect of inorganic salt concentration and types on electrophoretic migration of oil droplets in oil-in-water emulsion: A molecular dynamics study. *J. Mol. Liq.* **2022**, *367*, 120549.
(36) Wang, Y. D.; Li, S. Y.; Zhang, Y. W.; Zhang, Z. L.; Yuan, S. D.; Wang, D. Effect of electric field on coalescence of an oil-in-water emulsion stabilized by surfactant: a molecular dynamics study. *RSC Adv.* **2022**, *12*, 30658−30669.
(37) Qi, Z.; Sun, Z.; Li, N.; Chen, Q.; Liu, W.; Li, W.; Sun, J. Electrophoretic coalescence behavior of oil droplets in oil-in-water emulsions containing SDS under DC electric field: A molecular dynamics study. *Fuel* **2023**, *338*, 127258.
(38) Oliveira, N. F. B.; Pires, I. D. S.; Machuqueiro, M. Improved GROMOS 54A7 Charge Sets for Phosphorylated Tyr, Ser, and Thr to Deal with pH-Dependent Binding Phenomena. *J. Chem. Theory Comput.* **2020**, *16* (10), 6368−6376.
(39) Malde, A. K.; Zuo, L.; Breeze, M.; Stroet, M.; Poger, D.; Nair, P. C.; Oostenbrink, C.; Mark, A. E. An Automated Force Field Topology Builder (ATB) and Repository: Version 1.0. *J. Chem. Theory Comput.* **2011**, *7* (12), 4026−4037.
(40) Koziara, K. B.; Stroet, M.; Malde, A. K.; Mark, A. E. Testing and validation of the Automated Topology Builder (ATB) version 2.0: prediction of hydration free enthalpies. *J. Comput.-Aided Mol. Des.* **2014**, *28* (3), 221−233.
(41) Wander, M. C. F.; Shuford, K. L. Molecular Dynamics Study of Interfacial Confinement Effects of Aqueous NaCl Brines in Nanoporous Carbon. *J. Phys. Chem. C* **2010**, *114* (48), 20539−20546.
(42) Apostolakis, J.; Ferrara, P.; Caflisch, A. Calculation of conformational transitions and barriers in solvated systems: Application to the alanine dipeptide in water. *J. Chem. Phys.* **1999**, *110* (4), 2099−2108.
(43) Hess, B.; Kutzner, C.; van der Spoel, D.; Lindahl, E. GROMACS 4: Algorithms for Highly Efficient, Load-Balanced, and Scalable Molecular Simulation. *J. Chem. Theory Comput.* **2008**, *4* (3), 435−447.
(44) Darden, T.; York, D.; Pedersen, L. Particle mesh Ewald: An Nlog(N) method for Ewald sums in large systems. *J. Chem. Phys.* **1993**, *98* (12), 10089−10092.

https://doi.org/10.1021/acsomega.4c05623
ACS Omega 2024, 9, 48232−48245

(45) Essmann, U.; Perera, L.; Berkowitz, M. L.; Darden, T.; Lee, H.; Pedersen, L. G. A smooth particle mesh Ewald method. *J. Chem. Phys.* **1995**, *103* (19), 8577−8593.
(46) Shelley, J. C.; Sprik, M.; Klein, M. L. Molecular dynamics simulation of an aqueous sodium octanoate micelle using polarizable surfactant molecules. *Langmuir* **1993**, *9* (4), 916−926.
(47) De Lara, L. S.; Michelon, M. F.; Miranda, C. R. Molecular Dynamics Studies of Fluid/Oil Interfaces for Improved Oil Recovery Processes. *J. Phys. Chem. B* **2012**, *116* (50), 14667−14676.
(48) Kunieda, M.; Nakaoka, K.; Liang, Y.; Miranda, C. R.; Ueda, A.; Takahashi, S.; Okabe, H.; Matsuoka, T. Self-accumulation of aromatics at the oil-water interface through weak hydrogen bonding. *J. Am. Chem. Soc.* **2010**, *132* (51), 18281−18286.
(49) Song, S.; Zhang, H.; Sun, L.; Shi, J.; Cao, X.; Yuan, S. Molecular Dynamics Study on Aggregating Behavior of Asphaltene and Resin in Emulsified Heavy Oil Droplets with Sodium Dodecyl Sulfate. *Energy Fuels* **2018**, *32* (12), 12383−12393.
(50) Zhang, H.; Zhou, B.; Zhou, X.; Yang, S.; Liu, S.; Wang, X.; Yuan, S.; Yuan, S. Molecular dynamics simulation of demulsification of O/W emulsion containing soil in direct current electric field. *J. Mol. Liq.* **2022**, *361*, 119618.
(51) Wang, M.; Wang, L.; Zhang, T.; Xiao, N. Migration behavior of oil droplets and oil-water separation of an oil-in-water (O/W) emulsion in a DC electric field. *Beijing Huagong Daxue Xuebao* **2020**, *47* (5), 24−29.
(52) Huang, X.; He, L.; Luo, X.; Xu, K.; Lü, Y.; Yang, D. Charge-Transfer-Induced Noncoalescence and Chain Formation of Free Droplets under a Pulsed DC Electric Field. *Langmuir* **2020**, *36* (47), 14255−14267.

https://doi.org/10.1021/acsomega.4c05623
ACS Omega 2024, 9, 48232−48245